

Measuring Lipid Asymmetry in Planar Supported Bilayers by Fluorescence Interference Contrast Microscopy

Jonathan M. Crane, Volker Kiessling, and Lukas K. Tamm*

Department of Molecular Physiology and Biological Physics, University of Virginia, Charlottesville, Virginia 22908-0736

Received September 20, 2004. In Final Form: November 12, 2004

There is substantial scientific and practical interest in engineering supported lipid bilayers with asymmetric lipid distributions as models for biological cell membranes. In principle, it should be possible to make asymmetric supported lipid bilayers by either the Langmuir–Blodgett/Schäfer (LB/LS) or Langmuir–Blodgett/vesicle fusion (LB/VF) techniques (Kalb et al. *Biochim. Biophys. Acta* **1992**, *1103*, 307–316). However, the retention of asymmetry in biologically relevant lipid bilayers has never been experimentally examined in any of these systems. In the present work, we developed a technique that is based on fluorescence interference contrast (FLIC) microscopy to measure lipid asymmetry in supported bilayers. We compared the final degree of lipid asymmetry in LB/LS and LB/VF bilayers with and without cholesterol in liquid-ordered (l_o) and liquid-disordered (l_d) phases. Of five different fluorescent lipid probes that were examined, 1,2-dipalmitoyl-phosphatidylethanolamine-*N*-[lissamine rhodamine B] was the best for studying supported bilayers of complex composition and phase by FLIC microscopy. An asymmetrically labeled bilayer made by the LB/LS method was found to be at best 70–80% asymmetric once completed. In LB/LS bilayers of either l_o or l_d phase, cholesterol increased the degree of lipid mixing between the opposing monolayers. The use of a tethered polymer support for the initial monolayer did not improve lipid asymmetry in the resulting bilayer. However, asymmetric LB/VF bilayers retained nearly 100% asymmetric label, with or without the use of a tethered polymer support. Finally, lipid mixing across the center of LB/LS bilayers was found to have drastic effects on the appearance of l_d – l_o phase coexistence as shown by epifluorescence microscopy.

Introduction

Natural cell membranes are composed of lipid bilayers with asymmetric phospholipid compositions.¹ In the plasma membrane of the human erythrocyte, for example, >60% of all phosphatidylcholine (PC) and >80% of all sphingomyelin (SM) reside in the outer leaflet, while most of the phosphatidylethanolamine (PE), phosphatidylserine (PS), and phosphatidylinositol (PI) is found in the inner leaflet.^{2–4} There are several functional reasons and consequences of lipid asymmetry, which is why cells employ ATP-dependent translocases to move specific lipids to the desired face of the membrane.^{2–4} An increase in extracellular PS and PE has been correlated with cell death.^{3,4} Lipids involved in signaling events, such as PIP₂, are found only in the inner leaflet, where they interact specifically with tyrosine kinase receptors as part of G-protein-receptor-mediated signal transduction pathways.⁵ Several investigators have found evidence that the lipids in the outer leaflet (PC, SM, and cholesterol) of cell membranes are capable of segregating into domains, sometimes called “rafts”, of a more ordered lipid phase.^{6–8} Recent fluorescence studies in model membranes have

confirmed this *in vitro*,^{9–12} but so far attempts at reconstituting ordered lipid domains in model membranes that mimic the inner leaflet have failed.^{13,14} Still, others have suggested that rafts play a role in cell signaling,¹⁵ and lipid microdomains have also been cited as effectors of viral assembly.¹⁶ Cholesterol has been shown to cause clustering of soluble *N*-ethyl-maleimide-sensitive factor-attachment protein receptor (SNARE) proteins, but it is unclear whether this plays a role in SNARE-mediated exocytosis.¹⁷ Can ordered lipid domains in the outer leaflet influence these events that occur on the inner leaflet of the membrane? For PC/SM/cholesterol phase separation

* To whom correspondence should be addressed. E-mail: lkt2e@virginia.edu. Tel: (434) 982-3578. Fax: (434) 982-1616.

(1) Bretscher, M. S. Asymmetrical lipid bilayer structure for biological membranes. *Nat. New Biol.* **1972**, *236* (61), 11–12.

(2) Devaux, P. F. Static and dynamic lipid asymmetry in cell membranes. *Biochemistry* **1991**, *30* (5), 1163–1173.

(3) Boon, J. M.; Smith, B. D. Chemical control of phospholipid distribution across bilayer membranes. *Med. Res. Rev.* **2002**, *22* (3), 251–281.

(4) Quinn, P. J. Plasma membrane phospholipid asymmetry. *Subcell. Biochem.* **2002**, *36*, 39–60.

(5) Verkleij, A. J.; Post, J. A. Membrane phospholipid asymmetry and signal transduction. *J. Membr. Biol.* **2000**, *178* (1), 1–10.

(6) Simons, K.; Ikonen, E. Functional rafts in cell membranes. *Nature* **1997**, *387* (6633), 569–572.

(7) Brown, D. A.; London, E. Structure and function of sphingolipid- and cholesterol-rich membrane rafts. *J. Biol. Chem.* **2000**, *275* (23), 17221–17224.

(8) Anderson, R. G.; Jacobson, K. A role for lipid shells in targeting proteins to caveolae, rafts, and other lipid domains. *Science* **2002**, *296* (5574), 1821–1825.

(9) Dietrich, C.; Bagatolli, L. A.; Volovyk, Z. N.; Thompson, N. L.; Levi, M.; Jacobson, K.; Gratton, E. Lipid rafts reconstituted in model membranes. *Biophys. J.* **2001**, *80* (3), 1417–1428.

(10) Silviu, J. R. Fluorescence energy transfer reveals microdomain formation at physiological temperatures in lipid mixtures modeling the outer leaflet of the plasma membrane. *Biophys. J.* **2003**, *85* (2), 1034–1045.

(11) Baumgart, T.; Hess, T. S.; Webb, W. W. Imaging coexisting fluid domains in biomembrane models coupling curvature and line tension. *Nature* **2003**, *425*, 821–824.

(12) Crane, J. M.; Tamm, L. K. Role of cholesterol in the formation and nature of lipid rafts in planar and spherical model membranes. *Biophys. J.* **2004**, *86* (5), 2965–2979.

(13) Wang, T. Y.; Silviu, J. R. Cholesterol does not induce segregation of liquid-ordered domains in bilayers modeling the inner leaflet of the plasma membrane. *Biophys. J.* **2001**, *81* (5), 2762–2773.

(14) Crane, J. M.; Tamm, L. K. Cholesterol content and phospholipid asymmetry: Effect on raft formation in planar model membranes. *Biophys. J. Abstr.* **2003**, 1811-Pos.

(15) Baird, B.; Sheets, E. D.; Holowka, D. How does the plasma membrane participate in cellular signaling by receptors for immunoglobulin E? *Biophys. Chem.* **1999**, *82* (2–3), 109–119.

(16) Freed, E. O. Virology. Rafting with Ebola. *Science* **2002**, *296* (5566), 279.

to affect the inner leaflet of the plasma membrane, there must be an interaction between the two monolayers, but it is currently unknown whether the process is mediated by lipids or by transmembrane proteins.

One possible approach to studying interactions between opposing leaflets of a bilayer is to reconstitute model membranes of asymmetric compositions. This has proven to be a major challenge in the field. Recently, significant advances have been made in the endeavor to make asymmetric vesicles either by introducing novel synthetic translocases³ or by combining a lipid-coated inverted emulsion with a lipid monolayer at an oil–water interface.¹⁸ We prefer to use planar supported model membranes over vesicles because they can be made relatively quickly by either the Langmuir–Blodgett/Schäfer (LB/LS) method¹⁹ or a combined Langmuir–Blodgett/vesicle fusion (LB/VF) method²⁰ (see Materials and Methods). Once completed, details of the planar bilayer surface can be studied by epifluorescence microscopy or fluorescence recovery after photobleaching (FRAP). Another attractive feature of the LB/LS or LB/VF methods is that the individual monolayers and/or vesicles can be made with different lipid compositions. This was originally thought to result in an asymmetric bilayer, but new data suggest otherwise. Recent studies have utilized planar supported bilayers made by the LB/LS method to look at coexisting liquid phases of phospholipids and cholesterol.^{9,12,21} The goal of such investigations was to reconstitute ordered lipid domains under the microscope and possibly see if lipid–lipid interactions across the bilayer center could induce phase separation. We looked at planar bilayers made by the LB/LS method that were otherwise symmetric but stained only in the LS monolayer with a fluorescent lipid dye. To our surprise, we could see coexisting phases in both the proximal and distal leaflets.¹² The dye must have flipped across the membrane. [Nomenclature: The LB and LS monolayers are specifically those that existed separately on the solid support and at the air–water interface on the Langmuir trough, respectively, prior to contact, while the proximal and distal monolayers are the opposing leaflets of the resulting planar supported bilayer (see Materials and Methods)].

In addition to studying lateral lipid heterogeneity, our laboratory has a long-standing interest in using supported bilayers to examine reconstituted membrane proteins.^{22–25} It is particularly important to control the sidedness in

these systems, so that the globular domains of proteins have minimal contact with the solid substrate and are readily solvent accessible.

A common method for determining lipid asymmetry in vesicles is irreversible fluorescence bleaching by the addition of a reducing agent.^{18,26} Dithionite, which reduces the NBD fluorophore to a nonfluorescent compound, cannot pass the membrane barrier and therefore will only bleach fluorescent lipids in the outer leaflet. We attempted this approach in supported bilayers but found that dithionite permeates these model membranes, completely bleaching fluorescence in both leaflets of the bilayer (not shown). This is likely due to small defects in planar supported bilayers that cannot be seen under the light microscope.

To determine the degree of lipid asymmetry in supported bilayers, we have employed fluorescence interference contrast (FLIC) microscopy, a relatively new technique that was specifically designed for the study of membranes on solid supports.²⁷ It has long been hypothesized that a thin layer (1–3 nm) of water exists between a supported bilayer and the hydrophilic surface.^{19,28} The original purpose of FLIC was to determine the thickness of this water-filled cleft, and it has been successful in doing so for supported bilayers, attached giant vesicles, and adhered whole cells.^{29–32} We have recently extended the method to determine the distance between solid supports and polymer-supported bilayers, and even a fluorescently labeled SNARE protein complex reconstituted in a polymer-supported bilayer.³³ We show here that FLIC can also be used to determine lipid asymmetry in unevenly stained supported bilayers. In a symmetrically stained bilayer, the two faces of the membrane effectively constitute two layers of dye, each at a fixed distance from the silicon-oxide surface (Figure 1A). FLIC microscopy is used to determine the average distance of all dyes from the surface, which corresponds to the center of the membrane. A change in the average distance results in a left or right shift of the FLIC curve. If the bilayer is stained in only the proximal layer, for example, the average distance will be lower by one-half of the membrane thickness, and vice versa for a bilayer stained in only the distal monolayer (Figure 1B).

In the past, most FLIC experiments on supported bilayers have been carried out with DiIC₁₈ as the fluorescent probe. Since we want to examine the asymmetry of phospholipids in supported lipid bilayers, we first establish that various fluorescent phospholipid analogues in various lipid compositions produce the same average

(17) Lang, T.; Bruns, D.; Wenzel, D.; Riedel, D.; Holroyd, P.; Thiele, C.; Jahn, R. SNAREs are concentrated in cholesterol-dependent clusters that define docking and fusion sites for exocytosis. *EMBO J.* **2001**, *20* (9), 2202–2213.

(18) Pautot, S.; Frisken, B. J.; Weitz, D. A. Engineering asymmetric vesicles. *Proc. Natl. Acad. Sci. U.S.A.* **2003**, *100* (19), 10718–10721.

(19) Tamm, L. K.; McConnell, H. M. Supported phospholipid bilayers. *Biophys. J.* **1985**, *47* (1), 105–113.

(20) Kalb, E.; Frey, S.; Tamm, L. K. Formation of supported planar bilayers by fusion of vesicles to supported phospholipid monolayers. *Biochim. Biophys. Acta* **1992**, *1103* (2), 307–316.

(21) Stottrup, B. L.; Veatch, S. L.; Keller, S. L. Nonequilibrium behavior in supported lipid membranes containing cholesterol. *Biophys. J.* **2004**, *86* (5), 2942–2950.

(22) Kalb, E.; Tamm, L. K. Incorporation of cytochrome b5 into supported phospholipid bilayers by vesicle fusion to supported monolayers. *Thin Solid Films* **1992**, *210/211*, 763–765.

(23) Hinterdorfer, P.; Baber, G.; Tamm, L. K. Reconstitution of membrane fusion sites. A total internal reflection fluorescence microscopy study of influenza hemagglutinin-mediated membrane fusion. *J. Biol. Chem.* **1994**, *269* (32), 20360–20368.

(24) Wagner, M. L.; Tamm, L. K. Tethered polymer-supported planar lipid bilayers for reconstitution of integral membrane proteins: silane-polyethyleneglycol-lipid as a cushion and covalent linker. *Biophys. J.* **2000**, *79* (3), 1400–1414.

(25) Wagner, M. L.; Tamm, L. K. Reconstituted syntaxin1a/SNAP25 interacts with negatively charged lipids as measured by lateral diffusion in planar supported bilayers. *Biophys. J.* **2001**, *81* (1), 266–275.

(26) McIntyre, J. C.; Sleight, R. G. Fluorescence assay for phospholipid membrane asymmetry. *Biochemistry* **1991**, *30* (51), 11819–11827.

(27) Lambacher, A.; Fromherz, P. Fluorescence interference-contrast microscopy on oxidized silicon using a monomolecular dye layer. *Appl. Phys. A* **1996**, *63*, 207–216.

(28) Johnson, S. J.; Bayerl, T. M.; McDermott, D. C.; Adam, G. W.; Rennie, A. R.; Thomas, R. K.; Sackmann, E. Structure of an adsorbed dimyristoylphosphatidylcholine bilayer measured with specular reflection of neutrons. *Biophys. J.* **1991**, *59* (2), 289–294.

(29) Braun, D.; Fromherz, P. Fluorescence interference-contrast microscopy of cell adhesion on oxidized silicon. *Appl. Phys. A* **1997**, *65*, 341–348.

(30) Braun, D.; Fromherz, P. Fluorescence interferometry of neuronal cell adhesion on microstructured silicon. *Phys. Rev. Lett.* **1998**, *81*, 5241–5244.

(31) Fromherz, P.; Kiessling, V.; Kottig, K.; Zeck, G. Membrane transistor with giant lipid vesicle touching a silicon chip. *Appl. Phys. A* **1999**, *69*, 571–576.

(32) Lambacher, A.; Fromherz, P. Luminescence of dye molecules on oxidized silicon and fluorescence interference contrast microscopy of biomembranes. *J. Opt. Soc. Am. B* **2002**, *19*, 1435–1453.

(33) Kiessling, V.; Tamm, L. K. Measuring distances in supported bilayers by fluorescence interference-contrast microscopy: Polymer supports and SNARE proteins. *Biophys. J.* **2003**, *84* (1), 408–418.

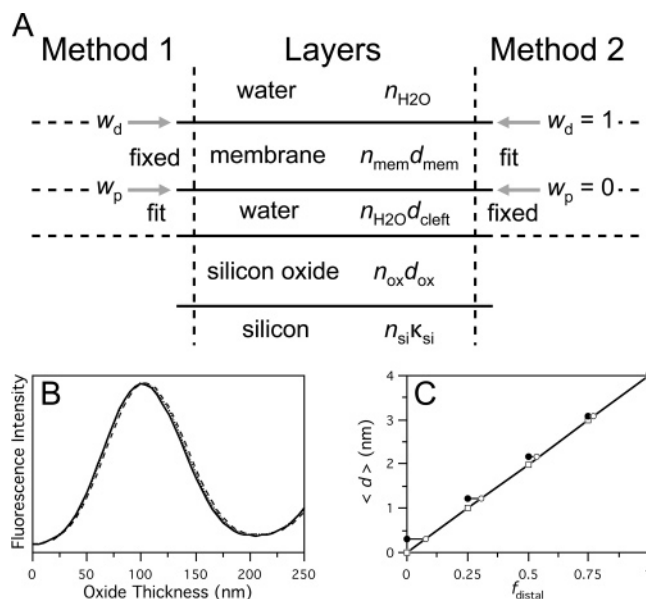


Figure 1. Optical layer model and fitting methods for symmetric and asymmetrically stained supported lipid bilayers. (A) Five layers are defined in the model (middle): silicon, with refractive index n_{si} and attenuation index κ_{si} ; silicon oxide, with refractive index n_{ox} and thickness d_{ox} ; a water-filled cleft with refractive index $n_{\text{H}_2\text{O}}$ and a thickness d_{cleft} ; the membrane, with refractive index n_{mem} and thickness d_{mem} ; and the bulk water layer with refractive index $n_{\text{H}_2\text{O}}$. The refractive indices of all materials are known (see Materials and Methods), and d_{ox} is predetermined by ellipsometry for each of up to 16 levels on a FLIC chip. Method 1 (left) is used with symmetrically stained bilayers or bilayers where the dye distribution is known. The positions of the fluorophores are entered into the fitting program as indicated by the arrows. Relative weights (w_{a} , w_{p}) are assigned for each position reflecting the known ratio of fluorescent lipids in the proximal and distal monolayers. d_{mem} is set at 4 nm for pure POPC bilayers and 4.5 nm for cholesterol-containing bilayers, and d_{cleft} is the one free parameter to be fit. Method 2 (right) is used with asymmetrically stained bilayers where the dye distribution is unknown. In this case, the fluorophor position is arbitrarily assigned as only in the distal face of the membrane ($w_{\text{a}} = 1$, $w_{\text{p}} = 0$), d_{cleft} is fixed at the value determined from symmetric experiments, and d_{mem} is the parameter to be fit. We call this the apparent membrane thickness $\langle d \rangle_{\text{exp}}$ because it approximates the average position of the fluorophores from the top of the cleft. The fraction of fluorescent lipids residing in the distal face of the membrane can be estimated by dividing $\langle d \rangle_{\text{exp}}$ by the actual membrane thickness. (B) Theoretical FLIC curves calculated for a POPC + 0.5% Rh-DPPE bilayer with all fluorophores in the distal monolayer (solid), fluorophores equally distributed between distal and proximal monolayers (dotted), or all in the proximal monolayer (dashed). (C) Plot of the fit apparent membrane thickness $\langle d \rangle_{\text{exp}}$ (●) and calculated average distance $\langle d \rangle$ (□) as a function of the actual fraction of fluorescent lipids in the distal face of the membrane f_{distal} (eqs 2 and 3). Open circles (○) represent the calculated f_{distal} from the fits without correction, and the black bars represent the errors in this calculation.

distances as DiIC₁₈ when measured by FLIC microscopy. We then determine the equilibrium position of dyes in asymmetrically stained LB/LS bilayers. Finally, we extend our study to LB/VF bilayers in both directly supported and tethered polymer-supported systems.

Materials and Methods

The following materials were purchased and used without further purification: 1-palmitoyl-2-oleoyl phosphatidylcholine (POPC), 1,2-dipalmitoyl phosphatidylcholine (DPPC), porcine brain PC, porcine brain SM, 1,2-dipalmitoyl phosphatidylethanolamine-*N*-[7-nitro-2-*l*,3-benzoxadiazol-4-yl] (NBD-DPPE), 1,2-dipalmitoyl phosphatidylethanolamine-*N*-[lissamine rhodamine

B] (Rh-DPPE), and 1,2-dioleoyl phosphatidylethanolamine-*N*-[lissamine rhodamine B] (Rh-DOPE) (Avanti, Alabaster, AL); 1,1'-didodecyl-3,3,3',3'-tetramethylindocarbocyanine perchlorate (DiIC₁₂) and 1,1'-dioctadecyl-3,3,3',3'-tetramethylindocarbocyanine perchlorate (DiIC₁₈) (Molecular Probes, Eugene, OR); cholesterol and *N*-[hydroxyethyl]piperazine-*N'*-[2-ethanesulfonic acid] (HEPES) (Sigma, St. Louis, MO); NaCl, NaOH, H₂SO₄, H₂O₂, methanol, chloroform, and Contrad detergent (Fisher Scientific, Fair Lawn, NJ). 1,2-Dimyristoyl phosphatidylethanolamine-*N*-[poly(ethylene glycol)-triethoxysilane] (DPS) was custom synthesized by Nektar Therapeutics (Huntsville, AL). Water was purified first with deionizing and organic-free filters (Virginia Water Systems, Richmond, VA) and then with a NANOpure system from Barnstead (Dubuque, IA) to achieve a resistivity of 18.2 MΩ/cm.

Large Unilamellar Vesicles (LUVs). The desired lipids were codissolved in chloroform or chloroform/methanol. Solvent was evaporated under a stream of N₂ followed by vacuum for at least 1 h. The resulting residue was resuspended in buffered saline (10 mM HEPES, 150 mM NaCl, pH = 7), rapidly vortexed, freeze-thawed 5 times by suspension in liquid N₂ followed by water at 40 °C, and extruded by 15 passes through two polycarbonate membranes with a pore diameter of 100 nm (Avestin, Ottawa, Ontario, Canada). Vesicles could be stored at 4 °C for up to 5 days prior to use.

FLIC Chips. The same FLIC chips were used as described previously.³³ Basically, silicon wafers were oxidized until the SiO₂ layer reached a thickness of 350 nm. The surface was then patterned by photolithography and HF etching to form either 4 or 16 distinct levels of oxide with thicknesses ranging from 10 to 330 nm. Oxide thicknesses were measured by microellipsometry. Immediately prior to use, the chips were cleaned in three volumes of 95% H₂SO₄ to one volume of 30% H₂O₂, followed by extensive rinsing in water.

Quartz Slides. Slides (40 mm × 25 mm × 1 mm) were purchased from Quartz Scientific (Fairport Harbor, OH). Slides were cleaned by boiling in Contrad detergent for 10 min and then hot bath sonication while still in detergent for 30 min, followed by extensive rinsing with water, methanol, and water again. Remaining organic residue was removed by immersion in three volumes of 95% H₂SO₄ to one volume of 30% H₂O₂, followed by extensive rinsing in water. Immediately prior to use, slides were further cleaned for 10 min in an argon plasma sterilizer (Harrick Scientific, Ossining, NY).

Planar Supported Bilayers. Planar supported bilayers were made by one of three methods: vesicle fusion, Langmuir–Blodgett/Schäfer, or combined Langmuir–Blodgett/vesicle fusion.

Vesicle Fusion. A clean FLIC chip was placed in a custom built flow-through chamber.³³ A 0.1 mM suspension of LUVs was injected into the chamber and incubated with the chip for 30 min to 1 h. Excess vesicles were washed out by extensive rinsing with buffered saline, leaving a single bilayer on the SiO₂ surface.

LB/LS. A lipid monolayer was spread from a chloroform solution onto a pure water surface in a Nima 611 Langmuir–Blodgett trough (Nima, Coventry, U.K.). The solvent was allowed to evaporate for 10 min, and the monolayer was compressed at a rate of 15 cm²/min to reach a surface pressure of 32 mN/m. A clean FLIC chip or quartz slide was then rapidly (200 mm/min) dipped into the trough and slowly (5 mm/min) withdrawn, while a computer maintained a constant surface pressure and monitored the transfer of lipids onto the substrate by measuring the change in surface area. The resulting monolayer on the solid support is known as the LB monolayer. A second monolayer was then spread and compressed in the same fashion as the first. This is the LS monolayer. The LB-coated substrate was attached to a suctioning tip, and its face was slowly lowered to contact the LS monolayer at the air/water interface to form a bilayer. Once contact was made, the substrate was pushed through the interface and onto the bottom half of the flow-through chamber underneath the surface. The chamber was then removed from the trough and sealed, and the water inside was exchanged for buffered saline by repeated rinsing.

LB/VF. An LB monolayer was formed on a FLIC chip and placed in the flow-through chamber. Vesicles were incubated with the LB-coated chip and rinsed as described above to form the bilayer.

Tethered Polymer-Supported Bilayers. A monolayer of 97% POPC and 3% DPS was spread on the trough,²⁴ and a FLIC chip was coated by the LB method as described above. The coated chip was placed in a desiccator to dry overnight. The triethoxysilane moiety of DPS was covalently linked to the SiO₂ surface (tethered) by baking in a 70 °C oven for 40 min. The chip was then returned to the desiccator to cool to room temperature, and a second monolayer (no DPS) was applied either by the LS or VF method.

Epifluorescence Microscopy. We used a Zeiss Axiovert 35 fluorescence microscope (Carl Zeiss, Thornwood, NY) with a mercury lamp as a light source and a 63× water immersion objective. Images were captured with a Cooke Sensicam QE charge-coupled device camera cooled to −12 °C (Cooke, Auburn Hills, MI). Bilayers stained with DiI or Rh-PEs were illuminated through a 546 nm band-pass filter (BP546/10, Schott Glaswerke, Mainz, Germany) and observed through a 610 nm band-pass filter (D610/60, Chroma, Brattleboro, VT). NBD-stained bilayers were illuminated through a 436 nm band-pass filter (D436/10, Chroma) and observed through a 535 nm band-pass filter (D535/40, Chroma).

FLIC Microscopy: Optical Parameters. The principles and theory of FLIC microscopy have been described in detail previously.^{27,32} We present a brief synopsis here to provide the reader with a basic idea of the method and introduce some terms.

Fluorescence interference arises from the phase difference between light waves arriving simultaneously at, or emitted simultaneously from, dye molecules that are at a fixed distance from a reflective surface. These phase differences are a function of the angles of the exciting and emitted waves with respect to the surface normal, the refractive index of the medium, the wavelength of exciting and emitted light, and the distance between the dye and the reflective surface. Therefore, all of these parameters affect the probability of excitation P_{ex} and emission P_{em} per unit time, as well as the rates of fluorescence decay k_f and nonradiative decay k_{nr} . The observed fluorescence intensity F is given by

$$F = \frac{1}{k_f + k_{\text{nr}}} P_{\text{ex}} P_{\text{em}} \quad (1)$$

P_{ex} , P_{em} , and k_f are expressed as functions of the angles of excitation and emission.³² These terms therefore depend on the numerical aperture of excitation NA_{ex} and emission NA_{em} of the objective and on the angles of orientation from the membrane (substrate) normal of the excitation and emission dipoles of the dye, θ_{ex} and θ_{em} , respectively. Finally, to account for changes in fluorescence lifetimes due to radiative and nonradiative processes, F also depends on the quantum yield Φ of the dye.

For incoming light at 546 nm, used to excite both Rh-PEs and DiI, we found that the effective NA_{ex} of our objective was 0.8 instead of the nominal value of 0.95.³³ However, $NA_{\text{ex}} = 0.95$ worked well for incoming light of 436 nm that was used to excite NBD. $NA_{\text{em}} = 0.95$ was used for emission at both wavelengths. For DiIC₁₈ in fluid lipid bilayers, it was previously determined that $\theta_{\text{ex}} = \theta_{\text{em}} = 62^\circ$, and $\Phi = 0.38$ provided good fits to the FLIC theory.³² However, due to slight differences in our microscopic setup, we found that these parameters had to be determined independently for all dyes and membrane environments, to get the best possible fits. This was done by selecting a subset of experimental data and performing fits to the FLIC theory while varying θ and Φ . The fitting procedure is discussed in the next section. The values that provided fits with the lowest errors were then used for further experiments. Table 1 shows θ and Φ as determined for each dye and lipid composition in this study.

FLIC Microscopy: Optical Layer Model. Figure 1A shows the optical layer model used in FLIC experiments. It consists of five layers: silicon, with refractive index $n_{\text{si}} = 4.904$ (435 nm), 4.138 (535 nm), 4.093 (545 nm), and 3.916 (610 nm) and attenuation index $\kappa_{\text{si}} = 0.143$ (435 nm), 0.036 (535 nm), 0.032 (545 nm), and 0.020 (610 nm);³⁴ silicon oxide of known thickness d_{ox} and refractive index $n_{\text{ox}} = 1.4696$ (435 nm), 1.4634 (535 nm),

1.4630 (545 nm), and 1.4605 (610 nm);³⁵ a thin water-filled cleft of thickness d_{cleft} and refractive index $n_{\text{H}_2\text{O}} = 1.333$; the supported membrane of thickness $d_{\text{mem}} = 4$ nm (POPC) and 4.5 nm (cholesterol-containing membranes)^{36,37} and refractive index $n_{\text{mem}} = 1.45$;³⁸ the bulk water between the membrane and the objective with refractive index $n_{\text{H}_2\text{O}}$. Therefore, the only free parameter is d_{cleft} , which has been determined by fitting FLIC data to this model in planar supported bilayers,^{32,33} attached giant unilamellar vesicles,^{31,32} and adhered whole cells.^{29,30,32} Headgroup-labeled dyes are used exclusively, and the dye position is assumed to be exactly at the membrane–water interface. Slight deviations from this assumption would introduce errors that are smaller than the experimental errors of the data.

We wanted to use FLIC to study asymmetrically stained planar membranes, so the model needed to be altered slightly to account for an uneven dye distribution in the two faces of the bilayer. We used two slightly different fitting methods depending on the system and question asked. Method 1 (Figure 1A, left) can be used for experiments where the bilayer is symmetrically stained or when the dye distribution is known with confidence. The fitting program allows the user to specify weighting factors for both the proximal (w_p) and distal (w_d) monolayer. A fit is then performed to determine d_{cleft} . Figure 1B shows theoretical curves for a POPC bilayer stained with Rh-DPPE either only in the distal monolayer ($w_d = 1$, $w_p = 0$, solid curve), equally in both monolayers ($w_d = 1$, $w_p = 1$, dotted curve), or only in the proximal monolayer ($w_d = 0$, $w_p = 1$, dashed curve). Method 2 (Figure 1A, right) can be used to determine the final dye distribution in asymmetrically stained membranes. In this case, we arbitrarily specify that all dyes reside in the distal monolayer ($w_d = 1$, $w_p = 0$), d_{cleft} is held constant at 2 nm (or 4 nm for polymer-supported bilayers),³³ and d_{mem} is the free parameter in the fit. The resulting apparent membrane thickness provides an estimated average distance ($\langle d \rangle$) of all dyes from the top of the cleft, which can then be converted to the fraction of dyes in the distal face of the bilayer f_{distal} by simply dividing by the actual membrane thickness:

$$f_{\text{distal}} = \langle d \rangle / d_{\text{mem}} \quad (2)$$

A systematic error arises from this treatment due to an understatement of the thickness of the membrane layer in the fitting model and a difference in the refractive indices of membrane and water. In actuality the membrane thickness does not change, but our fitting routine treats the membrane thickness in the optical model as a variable to reflect changes in the average dye position. The effect of this treatment can be exactly predicted, and the discrepancy between actual and fitted thickness is zero when $f_{\text{distal}} = 1$ ($\langle d \rangle = d_{\text{mem}}$) and maximum when $f_{\text{distal}} = 0$ ($\langle d \rangle \ll d_{\text{mem}}$). Figure 1C shows the correction factors between real and fitted values of $\langle d \rangle$ as a function of f_{distal} for a POPC bilayer stained with Rh-DPPE. These errors are small when compared with the statistical uncertainties arising from multiple FLIC experiments. Furthermore, the relationship between the experimentally fit distance $\langle d \rangle_{\text{exp}}$ and the actual average distance $\langle d \rangle$ is linear, which allowed us to correct for this error after the fits were completed:

$$\langle d \rangle = a \langle d \rangle_{\text{exp}} - b \quad (3)$$

The constants a and b depend on the wavelength of exciting and emitted light, the optical parameters θ and Φ , and the membrane thickness (Table 2).

(35) Landoldt, H.; Bornstein, R. *Numerical Data and Functional Relationships in Science and Technology*, 6th ed.; Springer: Berlin, 1962; Vol. 2.

(36) Franks, N. P. Structural analysis of hydrated egg lecithin and cholesterol bilayers. I. X-ray diffraction. *J. Mol. Biol.* **1976**, *100* (3), 345–358.

(37) Ipsen, J. H.; Mouritsen, O. G.; Bloom, M. Relationships between lipid membrane area, hydrophobic thickness, and acyl-chain orientational order. The effects of cholesterol. *Biophys. J.* **1990**, *57* (3), 405–412.

(38) Gingell, D.; Todd, I. Interference reflection microscopy. A quantitative theory for image interpretation and its application to cell-substratum separation measurement. *Biophys. J.* **1979**, *26* (3), 507–526.

(34) Jellison, G. E.; Modine, F. A. Optical constants for silicon at 300 and 10 K determined from 1.64 to 4.73 eV by ellipsometry. *J. Appl. Phys.* **1982**, *53*, 3745–3753.

FLIC Microscopy: Statistical Analysis. In a previous study, the limit of the accuracy of the distances determined by FLIC was on the order of 1–2 nm.³³ In those experiments, individual images were selected and intensities were entered into the fitting program by hand, which restricted the number of data sets that could be practically analyzed to around 10 per sample. We have now developed an automated intensity acquisition program using LabVIEW software (Nation Instruments, Austin, TX). An array of e.g. 8×8 square masks is overlaid onto the original image. The size of the squares is chosen to match the central part of the chip's terraces, thereby cropping the border areas. The intensity values of all pixels underlying each mask are then extracted. At this point thresholds can be applied to discard pixels that show extreme high (e.g., from dye aggregations) or low (e.g., from defects) intensities. From the remaining or all values, the mean and variance are determined assuming a normal distribution. All possible combinations of 16 (or 4 for 4-oxide chips) neighboring results are combined and saved in a format that can be used by the fitting software. With the 8×8 square masks on a 16-oxide chip, this results in 36 datasets of 16 means and errors. With 4-oxide chips, a 10×10 array of masks was used, which results in 81 datasets of 4 means and errors. The automatic extraction algorithm makes it possible to get a large number of data points, which improves the overall statistics and makes it easier to detect spatial results or error trends. In addition, using the results of one square in combination with all neighboring squares reduces the error originating from a slightly inhomogeneous illumination. In experiments with 16-oxide chips, 12–15 images were analyzed per sample, while only 6–8 images were analyzed per membrane on 4-oxide chips due to the larger number of datasets gathered from each image. At least two independently prepared bilayers were used for each composition reported in this study. The final column in Tables 1–3 (N) indicates the total number of data sets, with total images in parentheses.

Results

Symmetrically Stained LB/LS Bilayers. We first examined whether fluorescent lipid analogues other than DiIC₁₈ could be used to measure distances in supported bilayers. Symmetrically stained LB/LS bilayers on 16-oxide FLIC chips were used to determine the angle θ of the excitation and emission dipole and the quantum yield Φ of each fluorescent dye in membrane environments with different physical properties. We found that a θ of 62° and Φ of 0.64 provided the best fit in POPC bilayers with 0.5% DiIC₁₈ made by the LB/LS method, resulting in a d_{cleft} of 1.3 ± 0.8 nm (Figure 2A). DiIC₁₂ in POPC had similar optical properties ($\theta = 62^\circ$, $\Phi = 0.56$) and gave essentially the same cleft distance of 1.5 ± 0.7 nm (Figure 2B). We prefer headgroup-linked Rh-DOPE or Rh-DPPE to DiI for imaging of multiphase bilayers because they are phospholipids and therefore should better represent the behavior of unlabeled phospholipids and because they bleach more slowly. Both probes partition favorably into bilayer domains in the l_d phase.^{11,12} Both Rh-DOPE ($\theta = 68^\circ$, $\Phi = 0.85$) and Rh-DPPE ($\theta = 62^\circ$, $\Phi = 0.85$) yielded cleft distances of 2.3 ± 0.6 nm (Figure 2C and Table 1) in POPC bilayers. Finally, we examined NBD-DPPE, a dye that partitions favorably into l_o phase domains in multiphase bilayers.^{9,12} For 1% NBD-DPPE in POPC ($\theta = 55^\circ$, $\Phi = 0.88$), the cleft distance was 1.9 ± 0.5 nm (Figure 2D).

To represent a model l_o phase bilayer, we chose DPPC/cholesterol (1:1). For all five dyes tested, the different bilayer phase had a significant effect on the optical parameters (Table 1). DiIC₁₈ ($\theta = 73^\circ$, $\Phi = 0.64$) and DiIC₁₂ ($\theta = 70^\circ$, $\Phi = 0.73$) resulted in cleft distances of 0.2 ± 0.7 nm and 0.4 ± 0.8 nm, respectively, which were in marked disagreement with the previously determined values of ~ 2 nm. The reason for this discrepancy is unknown, but it could be the result of DiI being squeezed out from l_o

membranes into defects or grain boundaries with drastically altered positions of the dye in the membrane. Rh-DOPE, a doubly unsaturated lipid, did not properly incorporate into the highly ordered DPPC/cholesterol bilayers, so FLIC microscopy could not be performed. However, both fully saturated dyes, Rh-DPPE ($\theta = 90^\circ$, $\Phi = 0.85$) and NBD-DPPE ($\theta = 59^\circ$, $\Phi = 0.89$), incorporated well and gave distances of 2.0 ± 0.7 nm and 2.5 ± 0.9 nm, respectively, which are in good agreement with the cleft thicknesses measured in supported bilayers in the l_d phase (Table 1).

Motivated by our previous study of l_d – l_o phase coexistence in planar model membranes,¹² we attempted to use FLIC in LB/LS bilayers made from natural lipid mixtures. We chose brain PC/cholesterol (2:1) and brain SM/cholesterol (2:1) to represent l_d and l_o membranes, respectively. We compared these natural mixtures to synthetic analogues, POPC/cholesterol (2:1) and DPPC/cholesterol (2:1), which exhibit similar lateral diffusion properties as the natural analogues.¹² Surprisingly, the best-fit dipole angle θ of Rh-DPPE was much smaller in brain SM/cholesterol (68°) than in DPPC/cholesterol (90°) (Table 1). We also found that the standard deviation of the fit cleft distances was noticeably larger in the natural lipid mixtures than in the synthetic models (Table 1). Perhaps the chain composition variabilities in the natural mixtures led to an increased variance of the membrane thickness, which in turn led to a larger error in the average fit cleft distances. We therefore restricted our further studies to bilayers composed of synthetic lipids only.

Asymmetrically Stained LB/LS Bilayers. LB/LS bilayers of otherwise symmetric lipid composition were stained only in the LS monolayer, and the fraction of dye molecules retained in the distal monolayer f_{distal} of the resulting planar bilayer was determined as described in Materials and Methods (see Figure 1). Various lipid compositions and fluorescent dyes were tested, but in no case were we able to make a completely asymmetrically stained bilayer (Figure 3 and Table 2). Most asymmetry was retained in POPC stained with Rh-DOPE, with a final distal fraction of $78 \pm 14\%$. Rh-DPPE in POPC also remained fairly asymmetric ($70 \pm 15\%$, Figure 3A). DiIC₁₈ ($36 \pm 17\%$), DiIC₁₂ ($48 \pm 23\%$), and NBD-DPPE ($50 \pm 17\%$) were completely randomized in POPC bilayers.

Cholesterol was found to decrease the retained asymmetry in supported bilayers in both the l_o and l_d phases. Addition of 33% cholesterol resulted in a complete randomization of Rh-DPPE in POPC ($49 \pm 14\%$, Figure 3B). Similarly, the distal monolayer of DPPC/cholesterol (2:1) bilayers contained $67 \pm 13\%$ of the Rh-DPPE (Figure 3D), while only $52 \pm 12\%$ of the dye was found in the distal leaflet of DPPC/cholesterol (1:1) (Figure 3E). DPPC/cholesterol (1:1) retained $60 \pm 22\%$ of NBD-DPPE in the distal leaflet (Figure 3F). A recent study indicated that asymmetric LB/LS bilayers could be made using phospholipids in the gel phase;³⁹ however, pure DPPC bilayers could not be tested by FLIC because all fluorescent dyes are excluded from the gel phase during compression of the monolayer.¹²

Asymmetric Lipid Compositions and Staining. LB/LS supported bilayers composed of two monolayers with lipids in drastically different phases were randomized to a large extent with much lipid flip-flop occurring between the two leaflets. For example, an LB monolayer of DPPC joined with an LS monolayer of POPC + dye resulted in

(39) Liu, J.; Conboy, J. C. Direct measurement of the transbilayer movement of phospholipids by sum-frequency vibrational spectroscopy. *J. Am. Chem. Soc.* **2004**, *126* (27), 8376–8377.

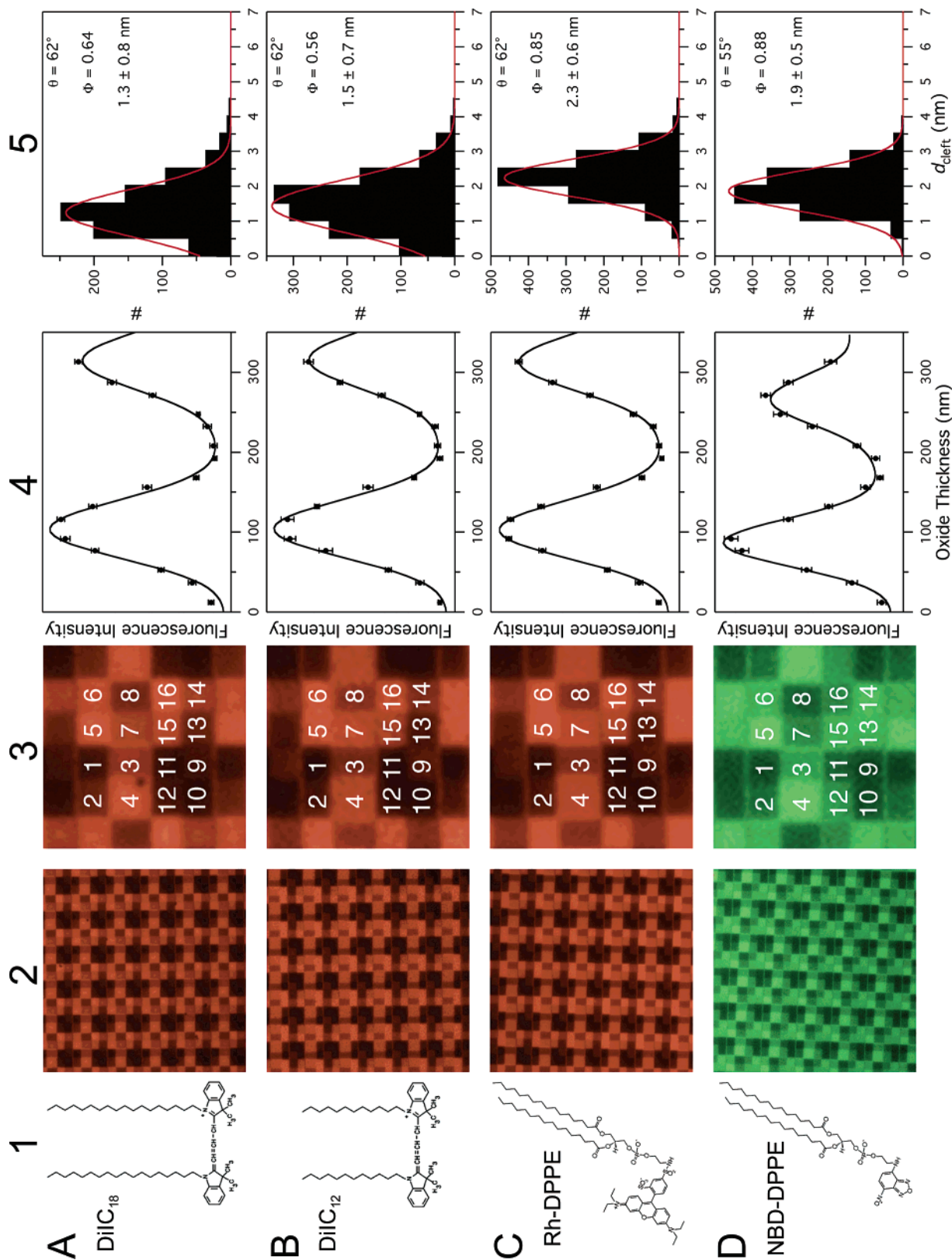


Figure 2. FLIC measurements of POPC bilayers prepared by the LB/LS method on 16-oxide FLIC chips and symmetrically stained with four different fluorescent lipids. Each row represents one of the following probes: (A) 0.5% DiIC₁₈, (B) 0.5% DiIC₁₂, (C) 0.5% Rh-DPPE, and (D) 1% NBD-DPPE. Columns from left to right: (1) Molecular structures of the fluorescent lipids, (2) Fluorescence micrographs of supported POPC bilayers on 16-oxide FLIC chips. Each square on a chip is 2.5 × 2.5 μm. (3) Close-ups of images 2 with numbers indicating the 16 different oxide levels. (4) Examples of FLIC fits where circles represent the experimental data from one set of 16 oxides, and the curve is the best fit to the theory. (5) Histograms of frequencies of resulting left thicknesses from multiple fits such as those shown in column 4. The curves are Gaussian fits to the histograms to confirm a normal distribution of the data. The means and standard errors of the d_{left} and the optical parameters θ and ϕ are shown in each panel. See Table 1 for complete results.

Table 1. Optical Fitting Parameters and Resulting Cleft Thicknesses for Symmetrically Stained LB/LS Bilayers Directly Supported on 16-Oxide FLIC Chips

dye	bilayer	θ (deg)	Φ	d_{mem} (nm)	d_{cleft} (nm)	N^a (m)
DiIC ₁₈	POPC	62	0.64	4.0	1.3 ± 0.8	852 (24)
DiIC ₁₈	DPPC/chol (1:1)	73	0.64	4.5	0.2 ± 0.7	851 (24)
DiIC ₁₂	POPC	62	0.56	4.0	1.5 ± 0.7	1290 (36)
DiIC ₁₂	POPC/chol (2:1)	69	0.82	4.5	0.0 ± 0.6	858 (24)
DiIC ₁₂	DPPC/chol (1:1)	70	0.73	4.5	0.4 ± 0.8	862 (24)
Rh-DOPE	POPC	68	0.85	4.0	2.3 ± 0.7	1005 (28)
Rh-DPPE	POPC	62	0.85	4.0	2.3 ± 0.6	1288 (36)
Rh-DPPE	POPC/chol (2:1)	70	0.85	4.5	2.3 ± 0.6	864 (24)
Rh-DPPE	DPPC/chol (2:1)	90	0.85	4.5	2.3 ± 0.6	861 (24)
Rh-DPPE	DPPC/chol (1:1)	90	0.85	4.5	2.0 ± 0.7	859 (24)
Rh-DPPE	bPC/chol (2:1)	67	0.85	4.5	2.4 ± 1.1	860 (24)
Rh-DPPE	bSM/chol (2:1)	68	0.85	4.5	2.3 ± 1.3	1077 (30)
NBD-DPPE	POPC	55	0.88	4.0	1.9 ± 0.5	1290 (36)
NBD-DPPE	DPPC/chol (1:1)	59	0.89	4.5	2.5 ± 0.8	854 (24)
NBD-DPPE	bPC/chol (2:1)	55	0.88	4.5	1.9 ± 1.2	1072 (30)
NBD-DPPE	bSM/chol (2:1)	55	1.0	4.5	1.7 ± 0.9	1077 (30)

^a N is the total number of data sets gathered from m images.

a supported bilayer with a large fraction of dark, irregularly shaped domains, which demonstrates that not only DiIC₁₂ but also DPPC and POPC must have mixed in this system (Figure 4A). The heterogeneous nature of these bilayers made FLIC analysis impossible. A similar

result was found when the LB monolayer was made in the l_o phase by adding 33% cholesterol (Figure 4B). However, when the same cholesterol content was used in both monolayers, bilayers without dark domains were obtained and FLIC experiments could be performed (Figure 4C). In these experiments, the LB monolayer was composed of DPPC/cholesterol (2:1), while the LS monolayer was composed of POPC/cholesterol (2:1), and both monolayers were individually stained with 0.5% Rh-DPPE in two separate trials. Regardless of which monolayer that was stained, θ was found to be 75°, and f_{distal} was about 60% (Figure 4D,E, Table 2).

4-Oxide FLIC Chips, Polymer Supports, and LB/VF Bilayers. We have previously shown that POPC bilayers made by vesicle fusion and stained with 0.5% DiIC₁₈ had the same fit cleft distance when measured on either 16-oxide FLIC chips with $2.5 \times 2.5 \mu\text{m}$ terraces or on 4-oxide FLIC chips with $5 \times 5 \mu\text{m}$ terraces. We also found that tethered DPS(poly(ethylene glycol))-supported bilayers could be made only on the 4-oxide FLIC chips with the larger terraces and that the polymer increased the cleft distance to about 4 nm.³³ Figure 5 shows that the same result was obtained when 0.5% Rh-DPPE was used as a fluorescent dye: the distance increased from 2.0 ± 0.8 nm to 4.1 ± 0.8 nm when the polymer was included.

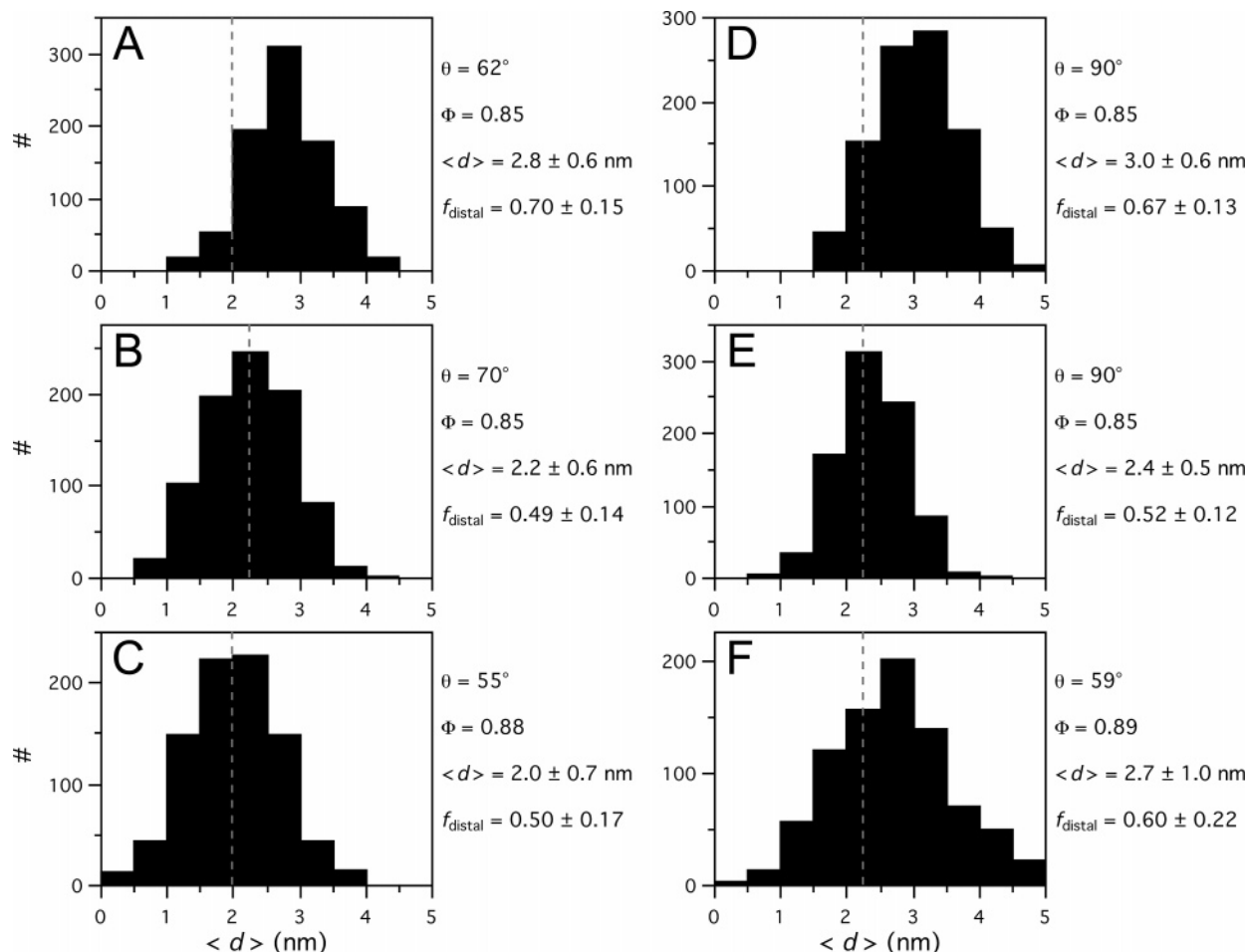


Figure 3. Asymmetry of fluorescent lipids retained in LB/LS bilayers in the l_d or l_o phase and asymmetrically stained with Rh-DPPE or NBD-DPPE. The histograms show the corrected $\langle d \rangle$ (eq 3) resulting directly from the FLIC fits. The fraction of dyes in the distal monolayer f_{distal} was calculated by dividing $\langle d \rangle$ by the known membrane thickness (eq 2). In each case, the LB monolayer was the same as the LS but contained no fluorescent probe, while the LS monolayer was composed as follows: (A) POPC + 0.5% Rh-DPPE, (B) POPC/cholesterol (2:1) + 0.5% Rh-DPPE, (C) POPC + 1% NBD-DPPE, (D) DPPC/cholesterol (2:1) + 0.5% Rh-DPPE, (E) DPPC/cholesterol (1:1) + 0.5% Rh-DPPE, and (F) DPPC/cholesterol (1:1) + 1% NBD-DPPE. The dashed lines represent the middle of the membrane, corresponding to 50/50 distributions of fluorescent lipids in each monolayer. 16-Oxide chips were used in all experiments. See Table 2 for complete results.

Table 2. Correction Factors and Corrected Fitting Results for Asymmetrically Stained LB/LS Bilayers Directly Supported on 16-Oxide FLIC Chips

dye	LB monolayer	LS monolayer	a^a	b (nm) ^a	$\langle d \rangle$ (nm) ^b	f_{distal}^c	N^d (m)
DiIC ₁₈	POPC	POPC + dye	1.085	0.338	1.4 ± 0.7	0.36 ± 0.17	647 (18)
DiIC ₁₂	POPC	POPC + dye	1.084	0.337	1.9 ± 0.9	0.48 ± 0.23	1216 (34)
Rh-DOPE	POPC	POPC + dye	1.083	0.330	3.1 ± 0.6	0.78 ± 0.14	857 (24)
Rh-DPPE	POPC	POPC + dye	1.083	0.333	2.8 ± 0.6	0.70 ± 0.15	864 (24)
Rh-DPPE	POPC/chol (2:1)	POPC/chol (2:1) + dye	1.081	0.363	2.2 ± 0.6	0.49 ± 0.14	864 (24)
Rh-DPPE	DPPC/chol (2:1)	DPPC/chol (2:1) + dye	1.078	0.351	3.0 ± 0.6	0.67 ± 0.13	971 (27)
Rh-DPPE	DPPC/chol (1:1)	DPPC/chol (1:1) + dye	1.078	0.351	2.4 ± 0.5	0.52 ± 0.12	861 (24)
Rh-DPPE	DPPC/chol (2:1)	POPC/chol (2:1) + dye	1.081	0.363	2.8 ± 0.7	0.62 ± 0.16	824 (23)
Rh-DPPE	DPPC/chol (2:1) + dye	POPC/chol (2:1)	1.081	0.363	2.7 ± 0.8	0.60 ± 0.17	966 (27)
NBD-DPPE	POPC	POPC + dye	1.096	0.385	2.0 ± 0.7	0.50 ± 0.17	863 (24)
NBD-DPPE	DPPC/chol (1:1)	DPPC/chol (1:1) + dye	1.096	0.431	2.7 ± 1.0	0.60 ± 0.22	853 (24)

^a Determined from theoretical curves prior to fitting experimental data (see Figure 1C). ^b Experimental results, corrected using eq 3. ^c Experimental results, calculated with eq 2. ^d N is the total number of data sets gathered from m images.

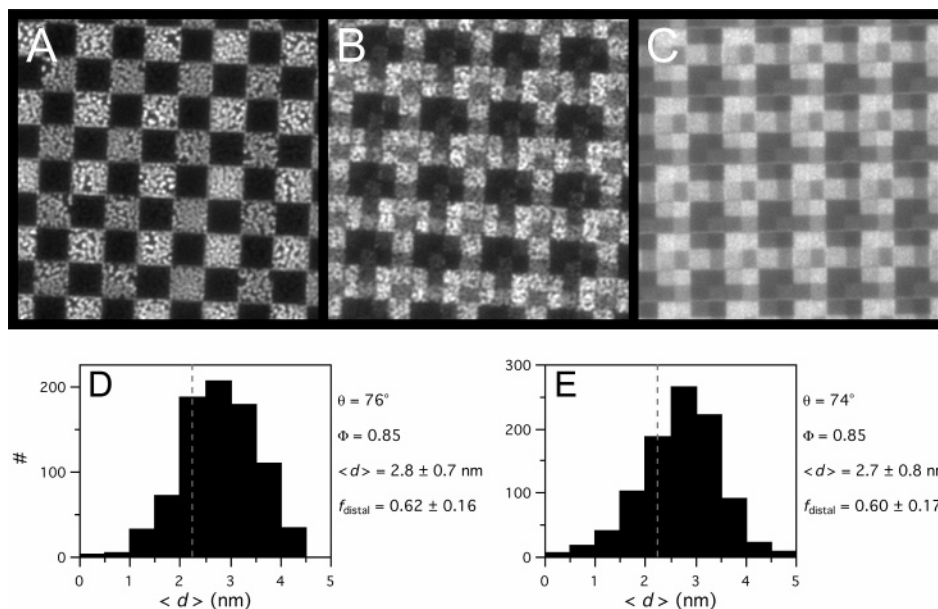


Figure 4. Asymmetrically stained LB/LS bilayers with asymmetric lipid compositions. (Top) Fluorescence micrographs of bilayers with the following compositions: (A) LB monolayer, DPPC; LS, POPC + 0.5% DiIC₁₂. (B) LB, DPPC/cholesterol (2:1); LS, POPC/cholesterol (2:1) + 0.5% Rh-DPPE. Each square on a 4- or 16-oxide FLIC chip is 5×5 or $2.5 \times 2.5 \mu\text{m}$, respectively. (Bottom) Histograms of corrected $\langle d \rangle$ (eq 3) and fitting results of FLIC data from bilayers with the following compositions: (D) LB monolayer, DPPC/cholesterol (2:1); LS, POPC/cholesterol (2:1) + 0.5% Rh-DPPE. (E) LB, DPPC/cholesterol (2:1) + 0.5% Rh-DPPE; LS, POPC/cholesterol (2:1). The fraction of fluorescent lipid retained in the distal monolayer f_{distal} was obtained from $\langle d \rangle$ by use of eq 2. The dashed lines represent the middle of the membrane, corresponding to 50/50 distributions of fluorescent lipids in each monolayer. See Table 2 for complete results.

Thus, neither the dye used nor the method of supported bilayer preparation, i.e., LB/VF vs LB/LS, changed this result.

Tethered polymer supports did not improve asymmetry in LB/LS bilayers. A polymer-supported POPC bilayer, stained only in the LS monolayer with 0.5% Rh-DPPE, retained only in the LS monolayer with 0.5% Rh-DPPE, retained 63 ± 31% of the dye in the distal leaflet (Table 3), i.e., a similar amount as POPC bilayers without the polymer support (70 ± 15%, Table 2).

However, almost completely asymmetrically stained bilayers could be made by the LB/VF method. When an unstained LB monolayer of POPC, either with or without a polymer support, was incubated with vesicles composed of POPC + 0.5% Rh-DPPE, the distal fraction of dye was found to be 97 ± 11% in directly supported bilayers, while the distal leaflet contained 84 ± 16% of the dye in the polymer-supported bilayers (Figure 6, Table 3). Just as with LB/LS bilayers, the polymer-supported bilayers retained slightly less asymmetry and had a larger standard error.

Asymmetry in LB/VF bilayers was found to be stable over long periods of time. In a directly supported POPC bilayer with a nearly 100% asymmetric dye distribution

immediately after the vesicle fusion step, >90% of the Rh-DPPE still resided in the distal monolayer after 2 h, and >80% after 6 h.

Asymmetrically Stained LB/LS Bilayers and Ordered Lipid Domains. Coexisting l_o and l_d phases have been visualized in supported lipid bilayers in the past.^{9,12} Phospholipid content and type, as well as cholesterol concentration, have a major effect on the fraction of membrane in either of the two coexisting phases. In some cases, asymmetrically prepared LB/LS bilayers have been examined, and conclusions have been drawn assuming that the contents of the opposing leaflets remain the same as in the initial monolayers. Having established that in fact significant fractions of the lipid species in the LB and LS monolayers mix during preparation, we sought to clarify the effect of asymmetric preparations on the observed liquid–liquid coexistence in both natural and synthetic lipid mixtures.

Figure 7A shows a supported lipid bilayer on a quartz support composed of POPC/DPPC/cholesterol (1:1:1), stained with 0.5% Rh-DPPE in the LS monolayer. The dye partitions into the disconnected l_d phase. It clearly stained both leaflets of the bilayer, indicating its ability

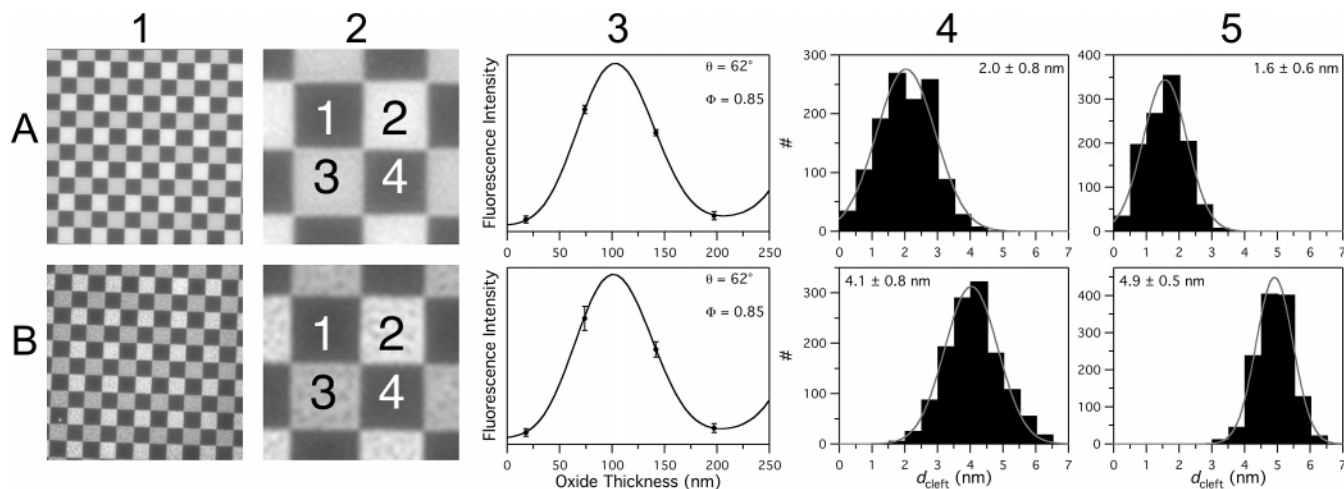


Figure 5. FLIC measurements of cleft distances between POPC bilayers (prepared by LB/LS or LB/VF methods) and solid supports measured on 4-oxide FLIC chips with or without tethered polymer supports. Each bilayer is composed of POPC in both layers and symmetrically stained with 0.5% Rh-DPPE. (A) Left to right: (1) Fluorescence micrograph of a LB/LS bilayer directly supported on a 4-oxide FLIC chip. Each square on the chip is $5 \times 5 \mu\text{m}$. (2) Close-up of image A1 indicating the 4 different oxide levels on the chip. (3) Example of a FLIC fit where circles represent experimental data and the curve represents the best fit to the data. (4) Histogram of fit cleft distances of POPC bilayers formed by the LB/LS method directly on 4-oxide FLIC chips. (5) Histogram of fit cleft distances of POPC bilayers formed by vesicle fusion directly to clean 4-oxide FLIC chips. (B) Left to right: (1) Fluorescence micrograph of a tethered DPS(poly(ethylene glycol))-supported bilayer prepared by the LB/LS method on a 4-oxide FLIC chip. (2) Close-up of image B1 indicating the 4 different oxide levels on the chip. (3) Example of a FLIC fit where circles represent experimental data and the curve represents the best fit to the data. (4) Histogram of fit cleft distances of tethered DPS-supported POPC bilayers formed by the LB/LS method on 4-oxide FLIC chips. (5) Histogram of fit cleft distances of tethered DPS-supported POPC bilayers formed by the LB/VF method on 4-oxide FLIC chips. The smooth curves are Gaussian fits to the histograms to confirm a normal distribution of the data. The means and standard errors are shown in each panel. See Table 3 for complete results.

Table 3. Fitting Results for Symmetric and Asymmetrically Stained Bilayers Made by Various Methods on 4-Oxide FLIC Chips

bilayer	method ^b	labeled	d_{cleft} (nm)	$\langle d \rangle$ (nm)	f_{distal}	N^c (m)
POPC	LB/LS	both	2.0 ± 0.8			1214 (15)
POPC + polymer ^a	LB/LS	both	4.1 ± 0.8			1293 (16)
POPC + polymer ^a	LB/LS	LS		2.5 ± 1.2	0.63 ± 0.31	1132 (14)
POPC	VF	vesicles	1.6 ± 0.6			1132 (14)
POPC	LB/VF	vesicles		3.9 ± 0.4	0.97 ± 0.11	1289 (16)
POPC + polymer ^a	LB/VF	both	4.9 ± 0.5			1255 (16)
POPC + polymer ^a	LB/VF	vesicles		3.4 ± 0.6	0.84 ± 0.16	1296 (16)

^a Polymer resides between the bilayer and the solid support (see Materials and Methods, ref 24). ^b LB, Langmuir–Blodgett; LS, Langmuir–Schäfer; VF, vesicle fusion. ^c N is the total number of data sets gathered from m images.

to flip into the proximal leaflet of the supported bilayer. Placing an LS monolayer of the same composition on top of an LB monolayer of pure POPC or POPC/cholesterol (2:1), both representing uniform l_d phases, did not significantly disrupt the appearance of the coexisting phases in the distal leaflet but did lead to more irregularly shaped l_d domains (Figure 7B,C). The lower contrast between the opposing phases indicates that the dye stained both leaflets in these cases as well, but the proximal leaflet contained no visible rafts. A drastically different result was obtained when we used an LB monolayer of either gel-phase DPPC or l_o phase DPPC/cholesterol (2:1). In both cases, the visible coexisting phases in the distal layer were completely abolished (Figure 7D,E).

Natural lipid mixtures showed similar but slightly different results. Planar bilayers of brain PC/brain SM/cholesterol (1:1:1) stained in the LS monolayer with 0.5% Rh-DPPE resulted in a bilayer with a connected l_o phase in one leaflet and a disconnected l_o phase in the opposing leaflet (Figure 7F). This shows that an equimolar mixture

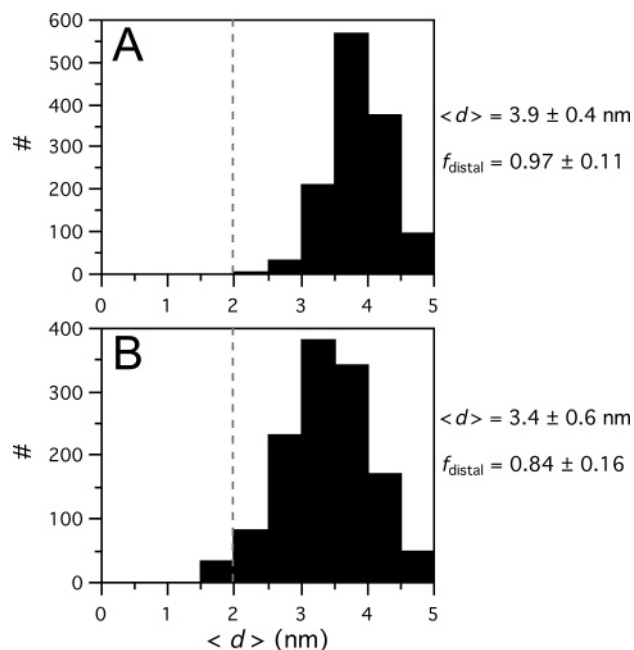


Figure 6. Asymmetry of fluorescent lipids retained in POPC bilayers prepared by the LB/VF method with or without a polymer support and asymmetrically stained with Rh-DPPE. (A) POPC + 0.5% Rh-DPPE vesicles fused to POPC LB monolayers directly deposited on 4-oxide FLIC chips. (B) POPC + 0.5% Rh-DPPE vesicles fused to tethered DPS-supported POPC monolayers on 4-oxide FLIC chips. The histograms show the corrected $\langle d \rangle$ (eq 3) resulting directly from FLIC fits. The fraction of fluorescent lipid retained in the distal monolayer f_{distal} was obtained from $\langle d \rangle$ by use of eq 2. The dashed lines represent the middle of the membrane, corresponding to 50/50 distributions of fluorescent lipids in each monolayer. See Table 3 for complete results.

of these lipids is very near the percolation threshold, i.e., the point where l_d phases become disconnected and l_o phases become connected.¹² Just as with the synthetic

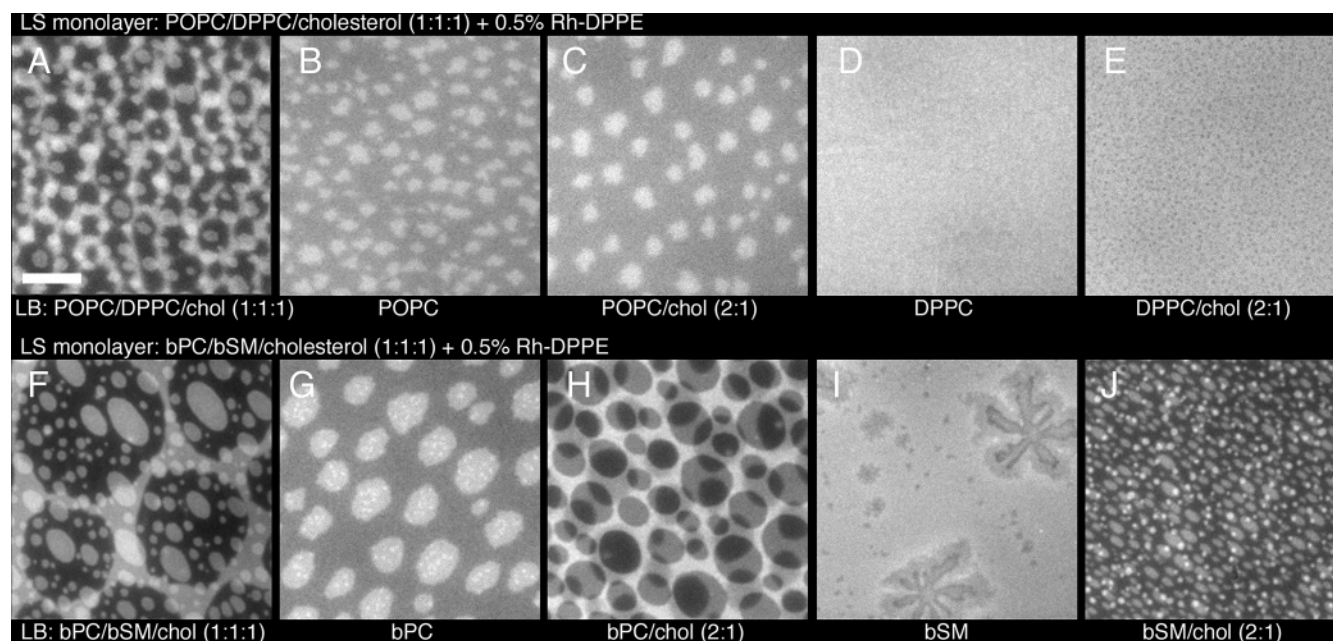


Figure 7. l_a - l_o phase coexistence in bilayers with asymmetric compositions. All bilayers were prepared by the LB/LS method on quartz supports. (A–E) The LS monolayer contained POPC/DPPC/cholesterol (1:1:1) + 0.5% Rh-DPPE, while the LB monolayer contained (A) POPC/DPPC/cholesterol (1:1:1), (B) POPC, (C) POPC/cholesterol (2:1), (D) DPPC, or (E) DPPC/cholesterol (2:1). (F–J) The LS monolayer contained bPC/bSM/cholesterol (1:1:1) + 0.5% Rh-DPPE, while the LB monolayer contained (F) bPC/bSM/cholesterol (1:1:1), (G) bPC, (H) bPC/cholesterol (2:1), (I) bSM, or (J) bSM/cholesterol (2:1). The bar represents 10 μm .

mixtures, replacing the brain PC/brain SM/cholesterol (1:1:1) LB monolayer with a monolayer of pure brain PC did not disrupt the coexisting phases in the LS monolayer, but it did result in less-rounded domains (Figure 7G). An LB monolayer of brain SM completely disrupted the visible coexisting phases of the LS monolayer. Large gel-phase domains, which were identical in shape and size to those seen before in pure brain SM bilayers,¹² were still visible in the proximal monolayer (Figure 7I). The contrast between these domains and the surrounding bilayer was less than previously observed for symmetric brain SM bilayers, probably because we are looking through the uniformly stained distal monolayer. An LB monolayer of either brain PC/cholesterol (2:1) or brain SM/cholesterol (2:1) drastically changed the appearance of the resulting bilayer. In both cases, the dye clearly has stained both leaflets, and the opposing leaflets have the same appearance, either above (Figure 7J) or below (Figure 7H) the percolation threshold. These experiments show that, at least in the situations of panels A, F, H, I, and J of Figure 7, significant lipid flip-flop takes place and, therefore, that caution is advisable when interpreting images of asymmetrically prepared bilayers showing lipid domains of coexisting phases.

Discussion

The ultimate goal of this work was to produce planar supported lipid bilayers with controlled asymmetric lipid compositions as models for cell membranes, which are composed of primarily phosphatidylcholine and sphingomyelin in the outer leaflet and phosphatidylethanolamine and various acidic lipid species in the inner leaflet. To achieve this goal, we first had to develop a technique that was capable of measuring lipid asymmetry in supported bilayers because it was clear from earlier studies that lipid flip-flop of varying degrees can occur during the preparation of asymmetric supported lipid bilayers. Since distances of fluorescent lipid analogues in supported lipid bilayers from the substrate surface can be measured by FLIC microscopy, we utilized and adapted this technique

to measure lipid asymmetry in supported lipid bilayers. To develop FLIC microscopy into a useful tool for measuring lipid asymmetry, we first had to determine which dyes are suitable for studying membranes with complex lipid compositions by FLIC microscopy. We then evaluated lipid asymmetry in bilayers made by both the LB/LS and LB/VF methods and found that only the LB/VF method, but not the LB/LS method, can retain full lipid asymmetry in supported bilayers under favorable conditions.

Finding The Right Dye. Prior to this study, most investigations with FLIC microscopy used DiI as the fluorescent lipid probe.^{27,29,30,32} Our initial studies show, however, that DiI interacts unfavorably with cholesterol-containing bilayers, producing unrealistically small cleft distances (Table 1). Although we do not know the real cause of this artifact, we hypothesize that DiI is excluded from interaction with equilibrated PC-cholesterol domains and complexes and may be squeezed out into microdefects of the bilayer. Alternatively, it may selectively interact with cholesterol and thus pull this component out of the bilayer equilibrium and form small lens defects within the membrane. Modeling of FLIC curves shows that an underestimate of the cleft distance will result if cholesterol causes the fluorescent headgroups to move toward the center of the membrane or if it is squeezed into microdefects in the bilayer (Figure 1A). Previously, DiI has been used to determine cleft thicknesses between cell membranes and FLIC chips.^{29,30} These membranes must have contained cholesterol as well, but unlike planar model membranes or vesicles, the plasma membranes of cells were stained after the bilayer had been formed. This prevented staining of the cytoplasmic leaflet, thereby removing the need for a second dye position in the optical layer model and thus reducing this source of error.

We found that fluorescent lipid analogues with fully saturated acyl chains, such as NBD-DPPE and Rh-DPPE, were best suited for studying bilayers of varying phases and cholesterol content (Table 1). NBD-DPPE partitions favorably into l_o and Rh-DPPE partitions favorably into

l_d phases.¹² Rh-DPPE emerges from these studies as the favorite probe for FLIC microscopy on supported membranes of complex composition. It incorporates well into all except gel-phase bilayers, it is bright, and it bleaches slowly.

Order Parameters and Dipole Orientation. Assuming that the acyl chains of the lipid probe are at a right angle to the chromophore, the order parameter S of the lipid acyl chains can be determined from the dipole orientation angle θ :³²

$$S = 1 - 3 \cos^2 \theta \quad (4)$$

Considering the chemical structure of DiI (Figure 2A,B), the assumption that the acyl chains are in fact perpendicular to the chromophore seems reasonable. Therefore, one calculates from $\theta = 62^\circ$ an acyl chain order parameter of 0.34 in l_d bilayers composed of POPC and an acyl chain order parameter of 0.65 in l_o bilayers composed of DPPC/cholesterol (1:1) ($\theta = 70^\circ$). For Rh-DOPE, Rh-DPPE, and NBD-DPPE, however, a single covalent bond exists between the chromophore and the lipid structure (Figure 2C,D). Therefore, the angle between the chromophore and acyl chains is more flexible and the chain order parameter is not readily determined from measurements of θ .

Making Asymmetric Supported Lipid Bilayers. We were unsuccessful in our numerous attempts to make fully asymmetrically stained LB/LS bilayers (Table 2). The reason why or the mechanism by which lipids in opposing monolayers mix is unknown. All reported data were acquired within minutes after completion of the bilayer, and examinations of bilayers several hours later showed no changes in the measured positions of the dyes. Lipid flip-flop in liposomes is known to occur on a time scale of many hours.⁴⁰ We therefore conclude that the flip-flop of fluorescent lipids from one side of the bilayer to the other must occur immediately upon contact between the monolayers at the air–water interface. The dried lipid film on the SiO₂ surface is probably significantly disrupted when it contacts the wet film on the trough. Large lateral pressure gradients must exist between the two leaflets upon contact. These pressure differences could allow material from the LS monolayer to mix with the LB monolayer. In many cases, this results in a complete randomization of fluorescent lipid probes between the two leaflets of the supported bilayer.

Despite the apparent mixing of components across LB/LS bilayers, coexisting liquid–liquid domains are not disrupted when the compositions of the opposing leaflets are symmetric (Figure 7A,G).¹² In fact, in our previous work we have avoided asymmetric lipid bilayers and used only symmetric ones to visualize the behavior of various raft lipid compositions. Furthermore, it has been shown that the general appearance of lipid domains in supported membranes is the same as at the air–water interface prior to immobilization on solid supports.²¹ Therefore, we originally hypothesized that l_o phase domains may not exchange lipids upon contact and that lipid mixing may be limited to the fluorescent-probe-containing l_d phases. To test this hypothesis, we measured lipid asymmetry in bilayers of varying cholesterol content and phase with fluorescent lipid probes that target both the l_d (Rh-DPPE) and l_o (NBD-DPPE) phases. Contrary to the original hypothesis, we found that l_o phases were just as susceptible to mixing as were the l_d phases in bilayers prepared by

the LB/LS method. In fact, cholesterol appears to even enhance lipid mixing in these bilayers (Figure 3, Table 2).

For many years, experiments have been carried out in this laboratory with planar supported bilayers made by a combined LB/VF technique.^{20,23–25,33,41–44} This method is often the only way to reconstitute transmembrane proteins and peptides into supported bilayers. We found that, unlike LB/LS bilayers, POPC bilayers made by the LB/VF method and stained with 0.5% Rh-DPPE only in the vesicles retained nearly 100% of the fluorescent lipids in the distal monolayer (Figure 6A, Table 3). Apparently, this method is gentle enough to that the initial LB monolayer remains fixed to the SiO₂ surface when it is incubated with the vesicle suspension. Previous work with LB/VF bilayers on quartz supports found that no fluorescence was lost when fluorescently labeled LB monolayers were exposed to buffered saline.²⁰ In this same work, the fluorescence intensity was reduced by only ~10% upon addition of unlabeled vesicle suspensions and completion of the bilayer. The current FLIC measurements confirm what was already suspected about the stability of the LB/VF bilayers from the earlier studies. Less than 10% of the lipid exchanges between opposing monolayers during the process of vesicle opening, fusion, and spreading. The LB/VF method is clearly less disruptive than the LB/LS method and, therefore, the preferred method to produce supported bilayers with asymmetric lipid composition. We find that POPC bilayers prepared by the LB/VF method retain a high degree of asymmetry for several hours after completion. Liu and Conboy also reported that supported bilayers can retain asymmetry for several hours.³⁹ However, they used bilayers formed in the gel phase and found that heating the system to temperatures near the main phase transition caused rapid flip-flop. In contrast, our POPC bilayers were always in the l_d phase and still managed to retain their asymmetry. It has previously been reported that heating a gel-phase supported bilayer causes the appearance of defects and budding of vesicles due to the expansion of the lipids.¹⁹ Liu and Conboy's sum-frequency vibrational method cannot distinguish between flip-flop and loss of lipids from the surface.

Tethered Polymer Supports. DPS is a lipid-anchored polymer that can be covalently linked to a SiO₂ surface and that provides a soft cushion to decouple planar membranes from the solid support. The poly(ethylene glycol) cushion provided by DPS has been shown to increase the lateral mobility of some integral membrane proteins in planar supported bilayers.^{24,25} FLIC microscopy confirms that the DPS support indeed lifts the membrane by about 2 additional nm in bilayers made by both the LB/LS or LB/VF methods (Figure 5).³³ This was previously only known for bilayers made by the direct vesicle fusion and LB/VF methods. Tethered DPS supports do not, however, improve the degree of lipid asymmetry when

(41) Tatulian, S. A.; Hinterdorfer, P.; Baber, G.; Tamm, L. K. Influenza hemagglutinin assumes a tilted conformation during membrane fusion as determined by attenuated total reflection FTIR spectroscopy. *EMBO J.* **1995**, *14* (22), 5514–5523.

(42) Gray, C.; Tatulian, S. A.; Wharton, S. A.; Tamm, L. K. Effect of the N-terminal glycine on the secondary structure, orientation, and interaction of the influenza hemagglutinin fusion peptide with lipid bilayers. *Biophys. J.* **1996**, *70* (5), 2275–2286.

(43) Han, X.; Steinhauer, D. A.; Wharton, S. A.; Tamm, L. K. Interaction of mutant influenza virus hemagglutinin fusion peptides with lipid bilayers: Probing the role of hydrophobic residue size in the central region of the fusion peptide. *Biochemistry* **1999**, *38* (45), 15052–15059.

(44) Tatulian, S. A.; Tamm, L. K. Secondary structure, orientation, oligomerization, and lipid interactions of the transmembrane domain of influenza hemagglutinin. *Biochemistry* **2000**, *39* (3), 496–507.

(40) Kornberg, R. D.; McConnell, H. M. Inside–outside transitions of phospholipids in vesicle membranes. *Biochemistry* **1971**, *10*, 1111–1120.

compared to directly supported membranes (Figure 6, Table 3). For both methods of preparation, the retained asymmetry of fluorescent lipid probes is slightly smaller in DPS-supported bilayers, and the uncertainties are somewhat larger. These larger errors could be the result of an increased flexibility and undulation motions in polymer-supported bilayers that are suppressed in directly supported bilayers. Alternatively or additionally, the frequency of small point defects may be increased in the polymer-supported bilayers. These defects may be caused by oxidation of lipids during the tethering process, where the initial monolayer is baked at 70 °C.

The Raft Conundrum. We have established that the LB/VF method is the only way to make supported bilayers, either with or without tethered polymer cushions, which are nearly completely asymmetric in lipid composition. Bilayers made by the LB/LS method are at most 70–80% asymmetric, and the addition of cholesterol further increases the mixing between monolayers. In addition, the variance in a sample of multiple distance measurements made by FLIC is generally larger in LB/LS bilayers than in bilayers made by the LB/VF or direct vesicle fusion methods (Figure 5, Table 3). Unfortunately, the LB/LS method is the only way to reconstitute ordered lipid domains on solid supports that are large enough to be viewed with a light microscope. As can be seen in Figure 7, the effects of asymmetrically constructed LB/LS bilayers on the size and shape of coexisting lipid domains are neither straightforward nor predictable. This confusion is exacerbated by the fact that we do not know exactly how much of each lipid resides in the respective monolayers.

Taken as a whole, the results presented in this work seem to erect a barrier to using planar supported bilayers to study lateral lipid heterogeneity in asymmetric systems. Indeed, we insist that all studies of LB/LS bilayers should be made with symmetric systems to ensure that the final composition be known. This comes at a time when increasing questions mount about the influence that ordered lipid microdomains have on the lipids and proteins on the inner leaflet of the plasma membrane.⁴⁵ There is hope, however, that a solution to this dilemma has already presented itself. Preliminary experiments have been performed using bilayers made by the LB/VF method with a lipid raft composition in the LB monolayer only, and fluorescently labeled in the vesicles only. In the resulting bilayer, coexisting phases in the proximal monolayer were visible, but the contrast was extremely low, indicating

that only a very small percent of the dye had stained the proximal monolayer (not shown). We envision this type of experiment to be useful in the future when studying the effect of l_a – l_o phase coexistence on reconstituted proteins. Such a system may mimic well the situation present in cells, where ordered lipid microdomains are suspected to exist in the outer leaflet of the plasma membrane, but signaling proteins interact with the membrane on the cytoplasmic side.

Acknowledgment. We thank Drs. Armin Lambacher and Peter Fromherz (Max Planck Institute for Biochemistry, Martinsried, Germany) for performing microellipsometry measurements, providing an improved version of the FLIC fitting software, and useful discussions.

Abbreviations

bPC	porcine brain phosphatidylcholine
bSM	porcine brain sphingomyelin
DiIC ₁₂	1,1'-didodecyl-3,3,3',3'-tetramethylindocarbocyanine perchlorate
DiIC ₁₈	1,1'-dioctadecyl-3,3,3',3'-tetramethylindocarbocyanine perchlorate
DPPE	1,2-dipalmitoyl phosphatidylcholine
DPS	1,2-dimyristoyl phosphatidylethanolamine- <i>N</i> -[poly(ethylene glycol)-triethoxysilane]
FLIC	fluorescence interference contrast
FRAP	fluorescence recovery after photobleaching
HEPES	<i>N</i> -[hydroxyethyl]piperazine- <i>N'</i> -[2-ethanesulfonic acid]
LB	Langmuir–Blodgett
LS	Langmuir–Schäfer
NBD-DPPE	1,2-dipalmitoyl phosphatidylethanolamine- <i>N</i> -[7-nitro-2-1,3-benzoxadiazol-4-yl]
PC	phosphatidylcholine
PE	phosphatidylethanolamine
PS	phosphatidylserine
PI	phosphatidylinositol
PIP ₂	phosphatidylinositol-bisphosphate
POPC	1-palmitoyl-2-oleoyl phosphatidylcholine
Rh-DOPE	1,2-dioleoyl phosphatidylethanolamine- <i>N</i> -[lissamine rhodamine B]
Rh-DPPE	1,2-dipalmitoyl phosphatidylethanolamine- <i>N</i> -[lissamine rhodamine B]
SM	sphingomyelin
SNARE	soluble <i>N</i> -ethyl-maleimide-sensitive factor-attachment protein receptor
VF	vesicle fusion
	LA047654W

(45) van Meer, G. Cell biology. The different hues of lipid rafts. *Science* **2002**, *296* (5569), 855–857.